Laser Light Scattering Studies of Soluble High-Performance Polyimides: Solution Properties and Molar Mass Distributions

Mohammad Siddiq,[†] Huizhen Hu,[‡] Mongxian Ding,[‡] Baozhang Li,[‡] and Chi Wu*[,†]

Department of Chemistry, The Chinese University of Hong Kong, N.T., Hong Kong, and Polymer Physics Laboratory, Changchun Institute of Applied Chemistry, Academia Sinica, Changchun, China

Received April 18, 1996; Revised Manuscript Received August 15, 1996[⊗]

ABSTRACT: Two soluble high-performance polyimides, poly(BCPOBDA/DMMDA) and poly(ODPA/DMMDA), in $CHCl_3$ at 25 °C have been studied using laser light scattering. We found that the *z*-average radius of gyration ($\langle R_g \rangle$) can be scaled to the weight-average molecular weight (M_w) as $\langle R_g \rangle$ (nm) = $4.95 \times 10^{-2} M_w^{0.52}$ and $\langle R_g \rangle$ (nm) = $1.25 \times 10^{-2} M_w^{0.66}$ respectively for poly(BCPOBDA/DMMDA) and poly(ODPA/DMMDA), indicating that poly(ODPA/DMMDA) in $CHCl_3$ at 25 °C has a more extended chain conformation than poly(BCPOBDA/DMMDA). Using the wormlike chain model approach, we found that the Flory characteristic ratios (C_∞) of poly(BCPOBDA/DMMDA) and poly(ODPA/DMMDA) are ∼20 and ∼31, respectively, indicating that both of them have a slightly extended chain conformation in comparison with typical flexible polymer chains, such as polystyrene, whose C_∞ is ∼10. A combination of the weight-average molar mass (M_w) with the translational diffusion coefficient distributions ($G(D)$) has led to D (cm²/s) = $3.53 \times 10^{-4} M^{-0.579}$ and D (cm²/s) = $4.30 \times 10^{-4} M^{-0.613}$ respectively for two soluble high-performance polyimides, poly(BCPOBDA/DMMDA) and poly(ODPA/DMMDA), in $CHCl_3$ at 25 °C. Using these two calibrations, we have successfully characterized the molar mass distributions of the two polyimides from their corresponding $G(D)$s. The exponents of these two calibrations further confirm that both of the polyimides have a slightly extended coil chain conformation in $CHCl_3$. The chain flexibility difference between these two polyimides has also been discussed.

Introduction

Polyimides, in particular those derived from fully aromatic monomers, represent a very important class of high-performance synthetic polymers because of their excellent mechanical, optical, and chemical properties.[1] It is well known that a fully thermoimidized polyimide is normally insoluble in common organic solvents. On the one hand, this insolubility leads to chemical resistance; on the other hand, this insolubility becomes a major obstacle in studying the solution properties, such as the chain flexibility and conformation. In the past, the solution properties and molecular parameters of these insoluble polyimides had to be estimated from their precursor, e.g., poly(amic acid) formed by the first-stage reaction of an aromatic diamine with an anhydride. This approach has some intrinsic and serious problems, including polyelectrolyte effects and the chain rigidity difference between a poly(amic acid) and its corresponding polyimide chain.[2−4] Moreover, information obtained from the study of those soluble poly(amic acids) can be strongly influenced by both the nature of imidazation and the reversible reaction.[5]

In order to tailor a polyimide to satisfy various specific requirements in industry, a careful examination and control of its chain conformation are of great importance. Practically, a correlation between the chain flexibility and bulk properties is still missing. Recently, we have made two soluble high-performance polyimides, poly[1,4′-bis(3,4-carboxyphenoxy)benzene dianhydride/2,2′-dimethyl-4,4′-methylenedianiline], termed poly(BCPOBDA/DMMDA), with a structure of

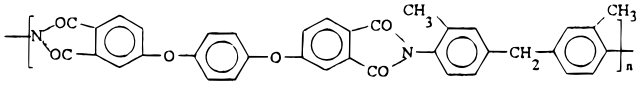

and poly[3,3′,4,4′-oxydi(phthalic anhydride)/2,2′-dimethyl-4,4′-methylenedianiline], termed poly(ODPA/DMMDA), with a similar structure of

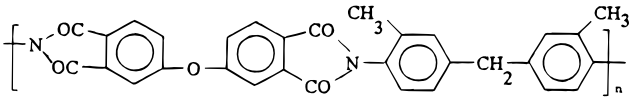

It is worth noting that poly(BCPOBDA/DMMDA) has two flexible ether linkages in its repeating unit, while poly(ODPA/DMMDA) has only one. Both of them are soluble in organic solvents such as chloroform ($CHCl_3$), dichloromethane (CH_2Cl_2), and dimethylacetamide (DMAc). This enhanced solubility provides us with an opportunity to directly study their solution properties. The Mark−Houwink equation of poly(BCPOBDA/DMMDA) in $CHCl_3$ at 25 °C, namely $[\eta] = 1.27 \times 10^{-1} M^{0.60}$, has been previously established.[6]

As for the characterization of the molar mass distributions of soluble polyimides, size exclusion chromatography (SEC; also known as GPC) is often used.[3] However, calibrating a SEC column is rather difficult. Moreover, each established calibration can only be used in a particular SEC instrument. Recently, coupling a small-angle light scattering detector with SEC has, in principle, solved this calibration problem. In this report, we will focus on the solution properties of poly(BCPOBDA/DMMDA) and poly(ODPA/DMMDA) and show an alternative laser light scattering method for the characterization of molar mass distributions of soluble polyimides.

* To whom correspondence should be addressed.
† The Chinese University of Hong Kong.
‡ Changchun Institute of Applied Chemistry.
⊗ Abstract published in *Advance ACS Abstracts,* October 1, 1996.

S0024-9297(96)00577-3 CCC: $12.00

Experimental Section

Sample Synthesis. Poly(BCPOBDA/DMMDA) was synthesized by polycondensation. Equal molar amounts of 1,4-bis(3,4-dicarboxyphenoxyl)benzene dianhydride (BCPOBDA) and 2,2′-dimethyl-4,4-methylenedianiline (DMMDA) were added in DMAc with a solid content of 15 wt %. A viscous solution was formed after an additional 2.5 equiv of acetic anhydride was added. The solution was stirred for 1 h and then 0.2 equiv of triethylamine as catalyst was added to start the imidization. At the end of the reaction, the solution was poured into ethanol to recover poly(BCPOBDA/DMMDA) from precipitation. After a successive washing of the precipitate with ethanol under heating, the final product was dried at 60 °C under vacuum until it reached a constant weight. Five fractions, labeled BD-1, BD-2, BD-3, BD-4, and BD-5, were used. Poly(ODPA/DMMDA) was also synthesized by this method except that 3,3′,4,4′-oxydi(phthalic anhydride) (ODPA) instead of BCPOBDA was used. Four poly(ODPA/DMMDA) fractions, labeled OD-1, OD-2, OD-3, and OD-4, were used. Fractionation was done by preparative gel permeation chromatography (GPC). Analytical grade chloroform was used as solvent without further purification. For each fraction, five solutions were prepared by dilution. The concentration was in the range ~4.0 × 10^{-4} to ~5.0 × 10^{-3} g/mL. All polyimide solutions were clarified at room temperature using a 0.22 or 0.1 μm Whatman filter, depending on the polymer size.

LLS Measurements. A modified commercial light scattering spectrometer (ALV/SP-125) equipped with an ALV-5000 multi-τ digital time correlator and a solid-state laser (ADLAS DPY 425II, output power ≈ 400 mW at λ_0 = 532 nm) as the light source was used. The primary beam was vertically polarized with respect to the scattering plane. The spectrometer was calibrated with toluene to make sure that the scattering intensity from toluene had no angular dependence in the range 6−154°. The details of the LLS instrumentation and theory can be found elsewhere.[7,8] All LLS measurements were done at 25.0 °C.

In static LLS, the angular dependence of the excess absolute time-averaged scattered intensity, known as the excess Rayleigh ratio, $R_{vv}(q)$, of a dilute polymer solution at concentration C (g/mL) and a relatively low scattering angle θ can be related to the weight-average molecular weight M_w as[9]

$$\frac{KC}{R_{vv}(q)} \approx \frac{1}{M_w}\left(1 + \frac{1}{3}\langle R_g^2\rangle q^2\right) + 2A_2C \qquad (1)$$

where $K = 4\pi^2 n^2 (dn/dC)^2/(N_A\lambda_0^4)$ and $q = (4\pi n/\lambda_0)\sin(\theta/2)$, with N_A, dn/dC, n, and λ_0 being Avogadro's number, the specific refractive index increment, the solvent refractive index, and the wavelength of light in vacuo, respectively. A_2 is the second virial coefficient, and $\langle R_g^2\rangle_z^{1/2}$ (or written as $\langle R_g\rangle$) is the root-mean-square z-average radius of gyration. Measuring $R_{vv}(q)$ at a set of C and q, we were able to determine M_w, $\langle R_g\rangle$, and A_2 from a Zimm plot which incorporates the extrapolations of $q \to 0$ and $C \to 0$ on a single grid.

In dynamic LLS, precise intensity−intensity time correlation functions $G^{(2)}(t,q)$ in the self-beating mode were measured and[7,8]

$$G^{(2)}(t,q) = \langle I(t,q)I(0,q)\rangle = A[1 + \beta|g^{(1)}(t,q)|^2] \qquad (2)$$

where q is the scattering vector, β is a parameter depending on the coherence of the detection, t is the delay time, $g^{(1)}(t,q)$ is a normalized first-order electric field time correlation function, and A is a measured baseline. It should be stated that A is not an adjustable parameter. Instead, we insisted on the agreement between A and the calculated baseline within 0.1%, which requires a careful (dust-free) solution preparation. For a polydisperse sample, $g^{(1)}(t,\theta)$ is related to the line width distribution $G(\Gamma)$ by

$$g^{(1)}(t,\theta) = \langle E(t,\theta)E^*(0,\theta)\rangle = \int_0^\infty G(\Gamma)e^{-\Gamma t}\,d\Gamma \qquad (3)$$

A Laplace inversion of $g^{(1)}(t,q)$ can lead to $G(\Gamma)$. The line width

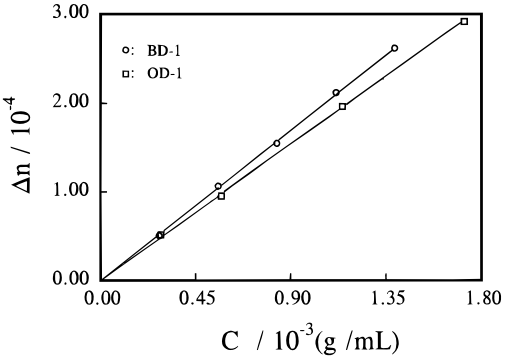

Figure 1. Typical plot of the refractive index increment (Δn) versus concentration (C) for poly(BCPOBDA/DMMDA) (○) and poly(ODPA/DMMDA (□) in $CHCl_3$ at T = 25 °C and λ_0 = 532 nm.

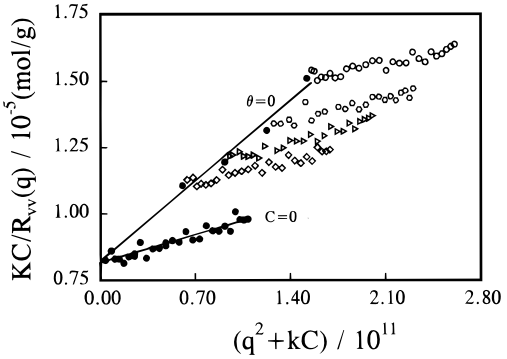

Figure 2. Typical Zimm plot for poly(BCPOBDA/DMMDA) (BD-3) in $CHCl_3$, where C ranges from 8.12 × 10^{-4} to 2.03 × 10^{-3} g/mL and k = 7.13 × 10^{13} mL/g.

Γ usually depends on both C and q as[10,11]

$$\Gamma/q^2 = D(1 + k_dC)(1 + f\langle R_g^2\rangle_z q^2) \qquad (4)$$

where D is the translational diffusion coefficient at $C \to 0$ and $q \to 0$, k_d is the diffusion second virial coefficient, and f, is a dimensionless parameter depending on the chain structure, solvent quality, and polydispersity. f increases as M_w decreases. The values of D, f, and k_d can be determined respectively from the extrapolations of $(\Gamma/q^2)_{c\to0,\theta\to0}$, $(\Gamma/q^2)_{c\to0}$ versus q^2 and $(\Gamma/q^2)_{q\to0}$ versus C.

Results and Discussion

Figure 1 shows the concentration dependence of the refractive index increment (Δn) of poly(BCPOBDA/DMMDA) and poly(ODPA/DMMDA) in $CHCl_3$ at 25 °C. The lines represent the least-squares fittings. The slopes of the lines lead to the specific refractive index increments (dn/dC). For poly(BCPOBDA/DMMDA) and poly(ODPA/DMMDA) in $CHCl_3$ at 25 °C, dn/dC = (0.189 ± 0.002) and (0.171 ± 0.002) mL/g, respectively. It should be stated that in this study the values of Δn were measured using a novel, high-precision differential refractometer, wherein the same laser light was shared by the refractometer and LLS, so that wavelength correction is not necessary.

Figure 2 shows a typical Zimm plot for poly(BCPOBDA/DMMDA) (BD-3) in $CHCl_3$, where C ranges from 8.12 × 10^{-4} to 2.03 × 10^{-3} g/mL. On the basis of eq 1, we were able to determine M_w, $\langle R_g\rangle$, and A_2 from the extrapolations of $[KC/R_{vv}(q)]_{q\to0,c\to0}$, $[KC/R_{vv}(q)]_{c\to0}$ versus q^2, and $[KC/R_{vv}(q)]_{q\to0}$ versus C, respectively, which are listed in Table 1. According to the wormlike chain model,[12] $\langle R_g^2\rangle = l^2\{^1/_3(L/l) - 1 + (2l/L) - (2l^2/L^2)[1 - \exp(-L/l)]\}$, where l is the persistence length and

Table 1. Summary of Static Laser Light Scattering Results of Poly(BCPOBDA/DMMDA) and Poly(ODPA/DMMDA) in $CHCl_3$[a]

fraction	M_w (g/mol)	$\langle R_g \rangle$ (nm)	A_2 (mol·cm^3/g^2)	l (nm)	C_∞
BD-1	3.45×10^5	39	9.2×10^{-4}	1.5	20
BD-2	2.15×10^5	30	1.2×10^{-3}	1.5	20
BD-3	1.24×10^5	25	1.6×10^{-3}	1.7	22
BD-4	9.04×10^4	20	2.3×10^{-3}	1.6	21
BD-5	5.07×10^4	14	2.8×10^{-3}	1.4	19
OD-1	3.00×10^4	13	9.0×10^{-4}	2.4	32
OD-2	2.50×10^4	11	1.0×10^{-3}	2.2	30
OD-3	1.80×10^4	<10	1.2×10^{-3}	2.4	32
OD-4	1.15×10^4	<10	1.4×10^{-3}	2.5	33

[a] Relative errors: M_w ±5%; $\langle R_g \rangle$, ±10%; A_2, ±15%; l and C_∞, ±15%.

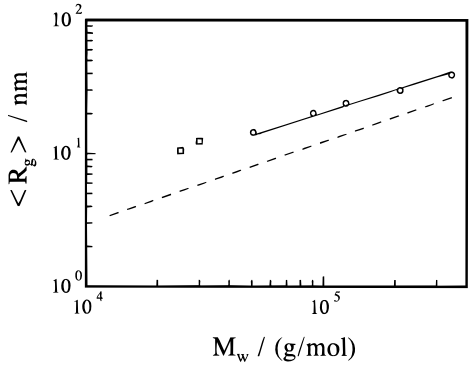

Figure 3. Double-logarithmic plot of $\langle R_g \rangle_z$ versus M_w for poly(BCPOBDA/DMMDA) (○) and poly(ODPA/DMMDA) (□), where the solid lines represent the least-squares fitting of $\langle R_g \rangle_z$ (nm) $= 4.95 \times 10^{-2} M_w^{0.52}$ and $\langle R_g \rangle_z$ (nm) $= 1.25 \times 10^{-2} M_w^{0.66}$, respectively. For comparison, the M_w dependence of $\langle R_g \rangle$ for polystyrene in toluene is also plotted (dashed line).

L ($=nl_u$) is the contour length; l_u and n ($=M_w/M_0$) are the projected length of the monomer unit and the average number of monomer units on each chain, respectively. For poly(BCPOBDA/DMMDA), $l_u \sim 2.5$ and $M_0 = 592$ g/mol, and for poly(ODPA/DMMDA), $l_u \sim 2.0$ nm and $M_0 = 500$ g/mol. Strictly speaking, $n = (M_z/M_w)(M_w/M_0)$ because $\langle R_g \rangle$ from static LLS is a z-averaged parameter. Using this model, we first calculated l using the measured $\langle R_g \rangle$ and the calculated L, and then the Flory characteristic ratio ($C_\infty = (2l/l_0) - 1$), where l_0 is the average bond length.[13] The estimated values of l and C_∞ of the polyimide fractions are summarized in Table 1, indicating that both poly(BCPOBDA/DMMDA) and poly(ODPA/DMMDA) have a more extended chain conformation than typical flexible polymers, such as polystyrene, whose l is ~1 nm. It is worth noting that for poly(BCPOBDA/DMMDA), $l_u > l$, whereas for poly(ODPA/DMMDA), $l_u < l$. The poly(ODPA/DMMDA) chain is even more extended because there is only one flexible ether linkage in its repeat unit. This extended chain conformation is expected because of the rigid aromatic groups in their backbones.

Figure 3 shows a double-logarithmic plot of $\langle R_g \rangle_z$ vs M_w for the two polyimides in $CHCl_3$ at 25 °C. The solid line represents the least-squares fittings of $\langle R_g \rangle_z$ (nm) $= 4.95 \times 10^{-2} M_w^{0.52}$ for poly(BCPOBDA/DMMDA). For comparison, we also list two data points of the OD-1 and OD-2 samples. The exponent value indicates that the poly(BCPOBDA/DMMDA) chain has a random-coil conformation in $CHCl_3$ at 25 °C. This coil conformation can be attributed to the flexible ether linkages in its monomer unit. Poly(ODPA/DMMDA) shows a similar behavior in $CHCl_3$ at 25 °C. For comparison, we also

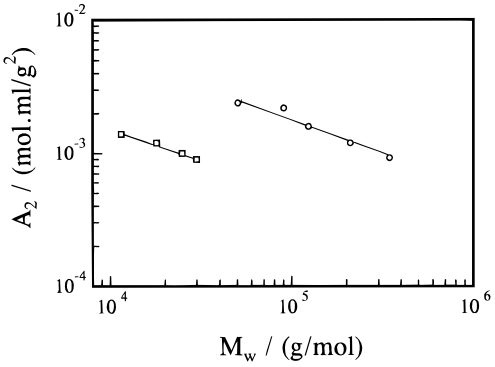

Figure 4. Double-logarithmic plot of A_2 vs M_w for poly(BCPOBDA/DMMDA) (○) and poly(ODPA/DMMDA) (□), where the lines respectively represent the least-squares fittings of A_2 (mL·mol/g^2) $= 5.42 \times 10^{-1} M_w^{-0.49}$ and A_2 (mL·mol/g^2) $= 1.10 \times 10^{-1} M_w^{-0.46}$

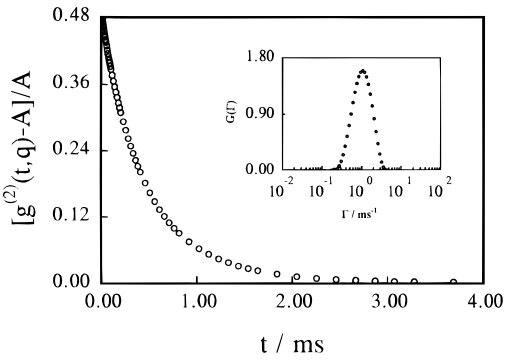

Figure 5. Typical measured intensity−intensity time correlation function $G^{(2)}(q,t)$ for poly(BCPOBDA/DMMDA) in $CHCl_3$ at $\theta = 20°$ and $T = 25$ °C. The inset shows the linewidth distribution $G(\Gamma)$ calculated from the Laplace inversion of $G^{(2)}(q,t)$.

plot the previously determined M_w dependence of $\langle R_g \rangle$ for polystyrene in toluene. It shows that for the same molecular weight the two polyimides have a more extended chain conformation.

Figure 4 shows a double-logarithmic plot of A_2 vs M_w for the two polyimides in $CHCl_3$ at 25 °C. The lines represent the least-squares fittings of A_2 (mL·mol/g^2) $= 5.42 \times 10^{-1} M_w^{-0.49}$ and $\langle A_2 \rangle$ (mL·mol/g^2) $= 1.10 \times 10^{-1} M_w^{-0.46}$ respectively for poly(BCPOBDA/DMMDA) and poly(ODPA/DMMDA). The exponent values are higher than ~0.25 predicted for typical random-coil polymer chains, which may reflect that these two polyimides have a more extended chain conformation in $CHCl_3$ at room temperature. It shows that poly(ODPA/DMMDA) in $CHCl_3$ has a much smaller A_2, or, in other words, poly(ODPA/DMMDA) is less soluble in $CHCl_3$ than poly(BCPOBDA/DMMDA), which may be related to the fact that the poly(ODPA/DMMDA) chain is more extended.

Figure 5 shows a typical plot of the measured intensity−intensity time correlation function for poly(BCPOBDA/DMMDA) in $CHCl_3$ at $\theta = 20°$ and $T = 25$ °C. The inset shows a typical $G(\Gamma)$ calculated from $G^{(2)}(t,q)$ using the Laplace inversion program (CONTIN).[14] On the basis of eq 4, we determined the average values of $\langle D \rangle$, $\langle f \rangle$, and $\langle k_d \rangle$ from the q and C dependence of the average line width $\langle \Gamma \rangle$ [$= \int_0^\infty G(\Gamma)\Gamma \, d\Gamma$]. The results are summarized in Table 2. The values of $\langle f \rangle$ (~0.1) agree well with those predicted for a random-coil polymer chain in a good solvent.[10,11] The small values of $\langle k_D \rangle$ (~20 mL/g) are expected because $k_d = 2A_2M_w - C_D N_A R_h^3/M_w$, and for $A_2 > 0$, the thermodynamic term

Table 2. Summary of Dynamic Laser Light Scattering Results and Molar Mass Distributions of Poly(BCPOBDA/DMMDA) and Poly(ODPA/DMMDA) in $CHCl_3$[a]

fraction	M_w (g/mol)	$\langle k_D \rangle$ (mL/g)	$\langle f \rangle$	$\langle D \rangle$ (cm^2/s)	$\langle R_g \rangle / \langle R_h \rangle$	$(M_w)_{calcd}$ (g/mol)	M_w/M_n	M_w/M_n
BD-I	3.45×10^5	~20	~0.1	1.93×10^{-7}	1.8	3.28×10^5	1.9	2.4_5
BD-2	2.15×10^5	~20	~0.1	2.57×10^{-7}	1.9	1.95×10^5	1.8_5	2.3
BD-3	1.24×10^5	~18	~0.1	3.19×10^{-7}	2.0	1.45×10^5	1.9	2.2
BD-4	9.05×10^4	~16	~0.1	4.39×10^{-7}	2.0	8.20×10^4	1.9	2.0
BD-5	5.07×10^4	~17	~0.1	5.82×10^{-7}	2.0	5.17×10^4	1.7	1.9
OD-1	3.00×10^4	~20	~0.1	7.32×10^{-7}	2.1	2.87×10^4	1.6	1.7
OD-2	2.50×10^4	~20	~0.1	8.15×10^{-7}	2.0	2.55×10^4	1.5	1.6
OD-3	1.80×10^4	~18	~0.1	9.15×10^{-7}		1.86×10^4	1.3	1.3_5
OD-4	1.15×10^4	~18	~0.1	1.33×10^{-6}		1.13×10^4	1.3	1.3

[a] Relative errors: M_w, ±5%; $\langle D \rangle$, ±1%; $\langle R_g \rangle / \langle R_h \rangle$, ±10%; M_w/M_n, ±10%.

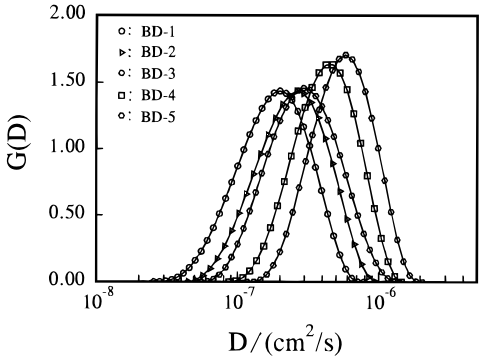

Figure 6. Translational diffusion coefficient distributions $G(D)$ of five poly(BCPOBDA/MMDA) fractions in $CHCl_3$ at T = 25 °C.

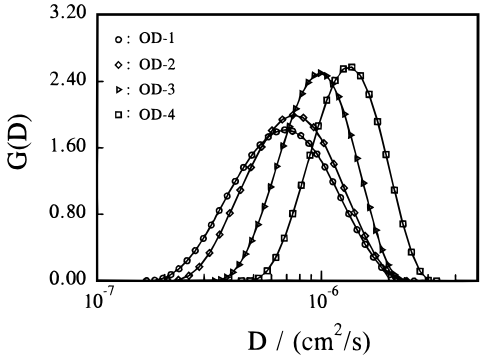

Figure 7. Translational diffusion coefficient distributions $G(D)$ of five poly(ODPA/DMMDA) fractions in $CHCl_3$ at T = 25 °C.

($2A_2M_w$) is partially canceled by the hydrodynamic term ($C_D N_A R_h^3/M_w$), where C_D is a positive constant.[11] Moreover, the partial specific volume also lowers the values of k_d. For these two polyimides in $CHCl_3$, $\Gamma \approx Dq^2$ because $(1 + k_dC)(1 + f\langle R_g^2 \rangle_z q^2) \sim 1$, which can be used to convert $G(\Gamma)$ to $G(D)$.

Figures 6 and 7 respectively show translational diffusion coefficient distributions $G(D)$ of five poly(BCPOBDA/DMMDA) fractions and four poly(ODPA/DMMDA) fractions. From each $G(D)$, we can calculate a hydrodynamic radius distribution, $f(R_h)$, and the average hydrodynamic radius, $\langle R_h \rangle$ [$= \int_0^\infty f(R_h) R_h \, dR_h$], by using the Stokes−Einstein equation, $D = k_BT/(6\pi\eta R_h)$, where k_B, T, and η are the Boltzmann constant, the absolute temperature, and the solvent viscosity, respectively. The values of $\langle D \rangle$ and $\langle R_g \rangle / \langle R_h \rangle$ are listed in Table 2. It is known that the ratio of the radius of gyration to the hydrodynamic radius reflects the chain conformation. The ratios of $\langle R_g \rangle / \langle R_h \rangle$ are close to the value (~1.84) predicted for random-coil polymer chains with a polydispersity index of $M_w/M_n \sim 2$ in a good solvent,[15] indicating that these two polyimides have a

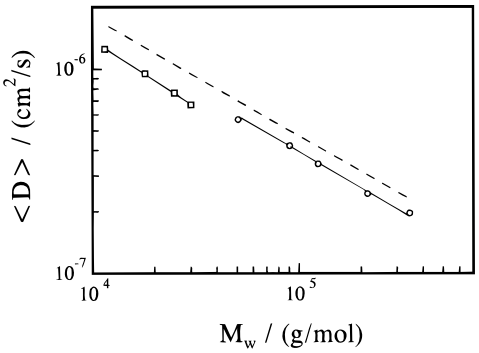

Figure 8. Double-logarithmic plots of $\langle D \rangle$ versus M_w for poly(BCPOBDA/DMMDA) (○) and poly(ODPA/DMMDA) (□), where the solid lines respectively represent the least-squares fittings of $\langle D \rangle$ (cm^2/s) = $2.28 \times 10^{-4} M_w^{-0.554}$ and $\langle D \rangle$ (cm^2/s) = $3.86 \times 10^{-4} M_w^{-0.62}$. For comparison, we also plot the data of polystyrene in toluene (dashed line).

coil chain conformation in solution. It is worth noting that for poly(BCPOBDA/DMMDA) in $CHCl_3$ $\langle R_g \rangle / \langle R_h \rangle$ increases slightly as M_w decreases. This is understandable because a polymer chain becomes more rigid when it is short.

Figure 8 shows a double-logarithmic plot of $\langle D \rangle$ versus M_w. The solid lines represent the least-sqares fittings of $\langle D \rangle = \langle k_D \rangle M_w^{-\langle \alpha_D \rangle}$ with $\langle k_D \rangle = 2.28 \times 10^{-4}$ and $\langle \alpha_D \rangle = 0.554$ for poly(BCPOBDA/DMMDA) and $\langle k_D \rangle = 3.86 \times 10^{-4}$ and $\langle \alpha_D \rangle = 0.620$ for poly(ODPA/DMMDA), where $\langle \, \rangle$ means that the values of $\langle k_D \rangle$ and $\langle \alpha_D \rangle$ were obtained from $\langle D \rangle$ and M_w rather than from D and M for monodisperse species. For poly(BCPOBDA/DMMDA), the value of $\langle \alpha_D \rangle = 0.554$ further indicates that it has a random-coil chain conformation, while for poly(ODPA/DMMDA) the slightly higher value of $\langle \alpha_D \rangle = 0.620$ implies that its chain is more extended in $CHCl_3$ at T = 25 °C. For comparison, we have also plotted the M_w dependence of $\langle D \rangle$ for polystyrene in toluene (the dashed line). It shows that for the same molar mass, polystyrene has a smaller hydrodynamic radius than the two polyimides, indicating a relatively more extended chain conformation of the two polyimides. Theoretically, with these calibrations, $G(D)$ can be transformed into a molar mass distribution, e.g., a differential weight distribution of molar mass, $f_w(M)$. The principle is outlined as follows. In static LLS, when $C \to 0$ and $q \to 0$

$$R_{vv}(\theta) \propto \langle I \rangle \propto \int_0^\infty f_w(M) M \, dM \tag{5}$$

On the other hand, in dynamic LLS

$$\langle E(t)E^*(0) \rangle_{t \to 0} = \int_0^\infty G(\Gamma) \, d\Gamma \propto \langle I \rangle \tag{6}$$

A comparison of eqs 5 and 6 leads to

$$\int_0^\infty G(\Gamma)\,\mathrm{d}\Gamma \propto \int_0^\infty G(D)\,\mathrm{d}D \propto \int_0^\infty f_w(M)M\,\mathrm{d}M \quad (7)$$

where $G(\Gamma) \propto G(D)$. Equation 7 can be rewritten as

$$\int_0^\infty G(D)D\,\mathrm{d}(\ln D) \propto \int_0^\infty f_w(M)M^2\,\mathrm{d}(\ln M) \quad (8)$$

where $\mathrm{d}(\ln D) \propto \mathrm{d}(\ln M)$. Therefore

$$f_w(M)M^2 \propto G(D)D \quad \text{or} \quad f_w(M) \propto \frac{G(D)D}{M^2} \quad (9)$$

With a pair of k_D and α_D, we can convert D to M and $G(D)$ to $f_w(M)$. One of the ways to verify such a molar mass distribution is to calculate its weight-average molar mass, $(M_w)_{calcld}$, and then compare it with M_w directly measured from static LLS. According to the definition of M_w and using eq 9, we have

$$(M_w)_{calcd} = \frac{\int_0^\infty F_w(M)M\,\mathrm{d}M}{\int_0^\infty F_w(M)\,\mathrm{d}M} = \frac{k_D^{1/\alpha_D}\int_0^\infty G(D)\,\mathrm{d}D}{\int_0^\infty G(D)D^{1/\alpha_D}\,\mathrm{d}D} \quad (10)$$

Our previous studies showed that using $\langle k_D\rangle$ and $\langle\alpha_D\rangle$ instead of k_D and α_D could introduce a large error in the calculated molar mass distribution.[16−18] In this study, we also found that when $\langle k_D\rangle$ and $\langle\alpha_D\rangle$ are used instead of k_D and α_D, $(M_w)_{calcd}$ is ~20−30% lower than M_w. Therefore, we have to adopt another way to find k_D and α_D, namely a combination of static and dynamic LLS results (i.e., M_w and $G(D)$) obtained from two or more polyimide fractions.

For N-number samples, we have N-number measured M_w and $G(D)$, denoted as $M_{w,i}$ and $G_i(D)$, where $i = 1$ to N. By assuming a pair of k_D and α_D and using eq 10, we can obtain N-number $(M_{w,i})_{calcd}$'s. For a given polymer sample, $(M_{w,i})_{calcd}$ should equal $M_{w,i}$, if both k_D and α_D are correctly chosen. Practically, by iterating k_D and α_D, we can find a pair of correct k_D and α_D to make $(M_{w,i})_{calcd} = M_{w,i}$ and minimize the right side of

$$\mathrm{ERROR} = \frac{1}{N}\sum_{i=1}^{N}\left[\frac{M_{w,i} - (M_{w,i})_{calcd}}{M_{w,i}}\right]^2 \quad (11)$$

In this way, we have avoided the polydispersity problem and used M_w as a constraint in the calculation.

Figure 9 shows a typical plot of the ERROR versus k_D at different values of α_D for poly(BCPOBDA/DMMDA). An overall minimum clearly defines a pair of k_D and α_D which leads to a calibration between D and M for monodisperse species. Using this method, we found that $k_D = 3.53 \times 10^{-4}$ and $\alpha_D = 0.579$ for poly(BCPOBDA/DMMDA) and $k_D = 4.30 \times 10^{-4}$ and $\alpha_D = 0.613$ for poly(ODPA/DMMDA). It is worth noting that the scaling constant $\alpha_{[\eta]}$ in the Mark−Houwink−Sakurada equation is ~0.6−0.7. Therefore, $3\alpha_D - 1 \approx \alpha_{[\eta]}$ just as predicted by Flory for a random-coil chain in a good solvent, indicating that both of the polyimides have a coil chain conformation and the poly(ODPA/DMMDA) chain is more extended because its α_D is slightly higher than that predicted for a random-coil chain in good solution. Using these two calibrations, we converted each $G(D)$ into a corresponding $f_w(M)$.

Figures 10 and 11 respectively show differential weight distributions of molar mass, $f_w(M)$, of different fractions of poly(BCPOBDA/DMMDA) and poly(ODPA/DMMDA). From each $f_w(M)$, we can calculate its weight-average molar mass $(M_w)_{calcd}$ and polydispersity index M_w/M_n, which are also listed in Table 2. $(M_w)_{calcd}$'s agree resonably with M_w's directly from static LLS. The values of M_w/M_n (≤ 2) are within the range predicted for polymers made by polycondensation. However, the values of M_w/M_n also indicate that the fractionation of poly(BCPOBDA/DMMDA) is less effective than that of poly(ODPA/DMMDA), which may be due to the fact that poly(BCPOBDA/DMMDA) is more soluble in $CHCl_3$ than poly(ODPA/DMMDA).

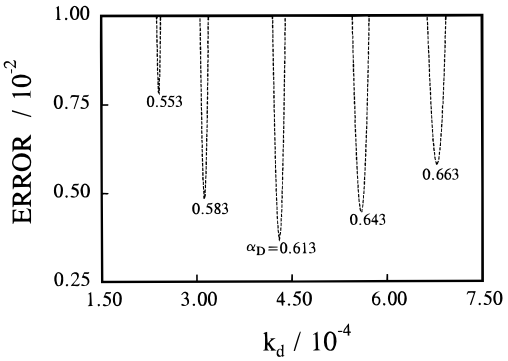

Figure 9. Plot of ERROR versus k_D at different values of α_D, where

$$\mathrm{ERROR} = \frac{1}{N}\sum_{i=1}^{N}\left[\frac{M_{w,i} - (M_{w,i})_{calcd}}{M_{w,i}}\right]^2$$

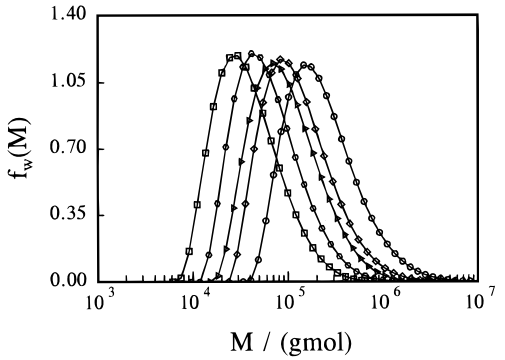

Figure 10. Differential weight distributions of molar mass of five poly(BCPOBDA/DMMDA) fractions, where the symbols are the same as in Figure 6.

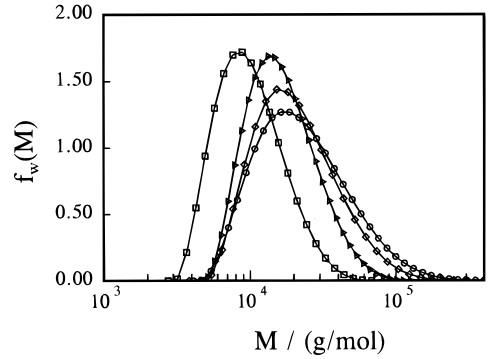

Figure 11. Differential weight distributions of molar mass of four poly(ODPA/DMMDA) fractions, where the symbols are the same as in Figure 7.

Conclusion

Laser light scattering studies of two soluble polyimides, poly(BCPOBDA/DMMDA) and poly(ODPA/DMMDA), have shown that both polyimides have a slightly extended coil conformation in $CHCl_3$ at 25 °C. The

positive A_2 values confirm that both poly(BCPOBDA/DMMDA) and poly(ODPA/DMMDA) are truly soluble in $CHCl_3$ at room temperature. Poly(ODPA/DMMDA) has a more extended chain conformation because it has only one ether linkage in its repeating unit, while poly(BCPOBDA/DMMDA) has two. The flexibility of these kinds of polyimides can be adjusted by introducing different numbers of the ether linkage. A combination of static and dynamic laser light scattering results, i.e., M_w and $G(D)$, leads to D (cm^2/s) $= 3.27 \times 10^{-4} M^{-0.579}$ and D (cm^2/s) $= 3.80 \times 10^{-4} M^{-0.613}$ respectively for two soluble polyimides, poly(BCPOBDA/DMMDA) and poly(ODPA/DMMDA), in $CHCl_3$ at 25 °C. Using these calibrations, we have successfully characterized the molar mass distributions of these two polyimides from their corresponding $G(D)$'s. The exponent values of the two calibrations further suggest that both of the polyimide chains are slightly extended in $CHCl_3$ at room temperature; in comparison, poly(ODPA/DMMDA) has a more extended chain conformation. In the future, using these two instrument-independent calibrations together with the A_2 values, we can quickly determine the molar mass distributions of these soluble polyimides from only one dynamic laser light scattering measurement of a dilute solution.

Acknowledgment. The financial support of this work by RGC (Research Grants Council of the Hong Kong Government) Earmarked Grants 1994/95 (CUHK A/C No. 221600260) is gratefully acknowledged. M. Siddiq wishes to acknowledge the Hong Kong Commonwealth Scholarship Commission (Hong Kong Government) for its generous financial support, which enabled him to finish his Ph.D. study at The Chinese University of Hong Kong. He also wishes to acknowledge Gomal University, Pakistan, for granting him the study leave.

References and Notes

(1) Li, F.; Kulig, J. J.; Kim, K. B.; Brittain, W. J.; Savitski, E. P.; Harris, F. W.; Cheng, S. Z. D. *J. Mater. Chem.* **1995**, *5*, 253.
(2) Wallach, M. L. *J. Polym. Sci., Part A* **1969**, *14*, 1995.
(3) Swanson, S. A.; Siemans, R.; Cotts, P. *Polyimides: Materials, Chemistry and Characterization*; Feger, C., Ed.; Elsevier Science: New York, 1989.
(4) Kim, S.; Cotts, P. M.; Volksen, W. *J. Polym. Sci., Polym. Phys. Ed.* **1992**, *30*, 177.
(5) Cotts, P. M.; Wolkensen, W.; Ferlin, S. *J. Polym. Sci., Polym. Phys. Ed.* **1992**, *30*, 373.
(6) Hu, H. Z.; Bo, S. Q.; Yuan, G. J.; Deng, M. X. *Chem. J. Chinese Univ.*, in press.
(7) Pecora, R.; Berne, J. *Dynamic Light Scattering*; Plenum Press: New York, 1976.
(8) Chu, B. *Laser Light Scattering, 2nd ed.*; Academic Press: New York, 1991.
(9) Zimm, B. H. *J. Chem. Phys.* **1948**, *16*, 1099.
(10) Stockmayer, W. H.; Schmidt, M. *Pure Appl. Chem.* **1982**, *54*, 407.
(11) Stockmayer, W. H.; Schmidt, M. *Macromolecules* **1984**, *17*, 509.
(12) Benoit, H.; Doty, P. *J. Phys. Chem.* **1953**, *57*, 958.
(13) Xu, Z.; Hadjichristidis, N.; Fetters, L. J.; Mays, J. W. *Adv. Polym. Sci.* **1995**, *120*, 1.
(14) Provencher, S. W. *J. Chem. Phys.* **1976**, *64* (7), 2772.
(15) Yamakawa, H. *Modern Theory of Polymer Solutions*; Harper and Row: New York, 1971.
(16) Wu, C. *Colloid Polym. Sci.* **1993**, *271*, 947.
(17) Wu, C. *J. Appl. Polym. Sci.* **1993**, *50*, 1753.
(18) Wu, C. *J. Polym. Sci., Polym. Phys. Ed.* **1994**, *32*, 803.

MA960577U